Steady-state magnetic field in the Alfvén resonance region

S. Rauf* and J. A. Tataronis
Department of Electrical and Computer Engineering, University of Wisconsin, Madison, Wisconsin 53706
(Received 8 May 1995)

The time-independent transverse magnetic field that is generated via the nonlinear mixing of linear Alfvén waves is examined in the vicinity of the Alfvén resonance surface. It is shown that this magnetic field is unidirectional, and it is confined within a narrow layer. The position of the layer along with the amplitude and direction of the magnetic field within it can be controlled by means of the primary wave frequency, wave numbers, and amplitude. Combinations of these magnetized layers can, therefore, be used for the modification or synthesis of transverse magnetic fields.

PACS number(s): 52.35.Bj, 52.35.Mw

I. INTRODUCTION

Steady-state current can be efficiently generated by the nonlinear mixing of linear Alfvén waves [1–5]. Previous studies have indicated that this current is considerably enhanced in regions where the derivatives of the field amplitudes are large. Keeping this in mind, we have examined the steady-state longitudinal current and the transverse magnetic field in the vicinity of the Alfvén resonance surface. Our results indicate that the leading-order current density is indeed significantly large in this region. It has, however, odd symmetry about the resonance surface and, in agreement with previous studies [6,7], the *total* current in the resonance region is zero. The major goal of this paper is to show that, even though the *total* current is zero, the current's characteristics are still very attractive for current drive related applications. This is primarily because of the transverse magnetic field that is generated by the steady-state current. It will be shown that this magnetic field is unidirectional and confined within a narrow layer about the Alfvén resonance surface. Since the position of this magnetized layer and the direction and amplitude of the field within it can be easily controlled externally, combinations of these layers can be used in alternative ways for a number of related applications. Among them, we mention here the synthesis of transverse magnetic fields with almost arbitrary profiles and the modification of already existing fields. These magnetized layers may also play an important role in the generation of magnetic fields in astrophysical and geophysical plasmas, where Alfvén waves abound. We will also show in the paper that viscosity leads to a broadening of the resonance layer and a flattening of the profile of the magnetic field within it.

II. PLASMA MODEL AND BASIC EQUATIONS

We study the problem in a slab geometry with Cartesian spatial coordinates $\tilde{x}$, $\tilde{y}$, and $\tilde{z}$. It is assumed that the plasma is cold and is governed by the equations of magnetohydrodynamics. It is also assumed that the equilibrium magnetic field $\tilde{\mathbf{B}}_0=B_0\hat{\mathbf{z}}$ is constant and directed parallel to the z axis, while the equilibrium density $\tilde{\rho}_0$ varies with $\tilde{x}$ only. Normalizing the governing plasma equations and combining them, we obtain the system

$$\rho\left[\frac{\partial \mathbf{v}}{\partial t}+(\mathbf{v}\cdot\nabla)\mathbf{v}\right]=(\nabla\times\mathbf{B})\times\mathbf{B}+\gamma\nabla^2\mathbf{v}\ , \tag{1}$$

$$\frac{\partial \mathbf{B}}{\partial t}=\nabla\times(\mathbf{v}\times\mathbf{B})+\epsilon\nabla^2\mathbf{B}\ , \tag{2}$$

where γ, ϵ, ρ, $\mathbf{v}$, and $\mathbf{B}$ are, respectively, the normalized viscosity, resistivity, plasma density, velocity, and magnetic field. The variables have been normalized in the following manner:

$$\mathbf{v}=\frac{\tilde{\mathbf{v}}}{v_A(\tilde{x}_0)}\ ,\quad \mathbf{B}=\frac{\tilde{\mathbf{B}}}{B_0}\ ,\quad \rho=\frac{\tilde{\rho}}{\tilde{\rho}_0(\tilde{x}_0)}\ ,\quad \epsilon=\frac{\eta\omega}{\mu_0 v_A^2(\tilde{x}_0)}\ ,$$

$$\gamma=\frac{\nu\omega}{\tilde{\rho}_0(\tilde{x}_0)v_A^2(\tilde{x}_0)}\ ,\quad t=\omega\tilde{t}\ ,\quad \mathbf{x}=\frac{\omega\tilde{\mathbf{x}}}{v_A(\tilde{x}_0)}\ ,$$

where $v_A(\tilde{x})=B_0[\mu_0\tilde{\rho}_0(\tilde{x})]^{-1/2}$ is the Alfvén speed, η is the unnormalized resistivity, ν is the unnormalized viscosity, ω is the frequency of the primary wave, and $\tilde{x}=\tilde{x}_0$ is the location of the Alfvén resonance surface. It should be noted that all variables with a tilde are unnormalized. Our goal in this study is to solve Eqs. (1) and (2) for the steady-state magnetic field that is generated by an externally excited Alfvén wave. To do so, we expand all the fields using the ordering scheme

$$u=u_0+\delta u_1 e^{i\psi}+\delta^2[u_2^{(0)}+u_2^{(2)}e^{2i\psi}]+\cdots+\text{c.c.}\ , \tag{3}$$

where $\psi=k_y y+k_z z-t$, δ is a small parameter related to the amplitude of the wave, u designates ρ or any component of $\mathbf{v}$ or $\mathbf{B}$, and $\mathbf{k}=k_y\hat{\mathbf{y}}+k_z\hat{\mathbf{z}}$ is the normalized wave vector with y and z components k_y and k_z, respectively. The frequency does not appear explicitly in the expression for ψ because of our normalization convention. In Eq. (3), $O(\delta)$ terms constitute the primary wave that is excited by the external antenna. The $O(\delta^2)$ terms are generated by the beating of these $O(\delta)$ quantities. Since the nonlinearities in the governing equations are quadratic in second order, the $O(\delta^2)$ terms are found at

*Present address: Department of Electrical and Computer Engineering, University of Illinois, Urbana, IL 61801.

zero and second harmonics of the fundamental frequency.

The $O(\delta)$ terms in the governing equations can be combined to obtain

$$A\mathbf{v}_1 = ik_z\hat{\mathbf{z}}(\nabla\cdot\mathbf{v}_1) + i\gamma\mathcal{L}\mathbf{v}_1 - \nabla(\nabla\cdot\mathbf{v}) + ik_z\nabla v_{z1} + i\epsilon\mathcal{L}(\rho_0\mathbf{v}_1) + \epsilon\gamma\mathcal{L}^2\mathbf{v}_1 , \quad (4)$$

where $A(x)=\rho_0(x)-k_z^2$ and $\mathcal{L}\equiv d^2/dx^2-k_y^2-k_z^2$. The magnetic field B_0 does not appear in the expression for A because of our normalization. If $\gamma=\epsilon=0$, it is well known that v_{x1} has a logarithmic singularity at the zeros of $A(x)$ [8]. Assuming that $A(x)=0$ at $x=x_0$, we define $x=x_0$ as the Alfvén resonance surface. From the z component of Eq. (4), we find that v_{z1} is independent of the other components. Since it does not play an important role in the dynamics of the problem, we let v_{z1} be zero in the rest of this analysis. Equation (4) can be solved for the first-order fields. These first-order components beat together with each other and generate secondary waves at zero and second harmonics of the fundamental frequency. The zero harmonic (steady-state) wave has a longitudinal current associated with it. To compute its density $J_{z2}^{(0)}$, we combine the $O(\delta^2)$ terms in the y component of Eq. (2) with

$$J_{z2}^{(0)} = \frac{\partial B_{y2}^{(0)}}{\partial x} , \quad (5)$$

which is the z component of the normalized Ampère law. After some algebraic manipulations, we find that

$$J_{z2}^{(0)} = -i[v_{x1}\mathcal{L}B_{y1}^* + v_{y1}^*\mathcal{L}B_{x1}] + \text{c.c.} \quad (6)$$

III. ANALYTICAL SOLUTION

Equations (4)–(6) comprise the basic tools that we use to analytically explore the characteristics of the steady-state current and magnetic field in the vicinity of the Alfvèn resonance surface. We first consider a purely resistive plasma with $\gamma=0$. Following Kappraff and Tataronis [9], we introduce a boundary layer about $x=x_0$ with a width of $O(\epsilon^{1/3})$. Outside the layer, resistive terms are not important and the x and y components of Eq. (4) can be combined to obtain

$$\frac{d}{dx}\left[\frac{A}{A-k_y^2}\frac{dv_{x1}}{dx}\right] + Av_{x1} = 0 . \quad (7)$$

The dominant term in the solution for v_{x1} is [8]

$$v_{x1} = C(\ln|x-x_0| + iM\pi) , \quad (8)$$

where C is an arbitrary constant, $M=0$ if $x<x_0$, $M=\text{sgn}(A_1)$ if $x>x_0$, and A_1 is defined in Eq. (9). To find the solution inside the layer, we introduce a scaled variable $\sigma=\epsilon^{-1/3}(x-x_0)$. We also expand the various components as follows [9]:

$$A = \epsilon^{1/3}\sigma A_1 + \epsilon^{2/3}\sigma^2 A_2 + \cdots , \quad (9)$$

$$\rho_0 = 1 + \epsilon^{1/3}\sigma\rho_{01} + \epsilon^{2/3}\sigma^2\rho_{02} + \cdots , \quad (10)$$

$$v_{x1} = v_{x10} + \epsilon^{1/3}v_{x11} + \epsilon^{2/3}v_{x12} + \cdots , \quad (11)$$

$$v_{y1} = \epsilon^{-1/3}v_{y10} + v_{y11} + \epsilon^{1/3}v_{y12} + \cdots . \quad (12)$$

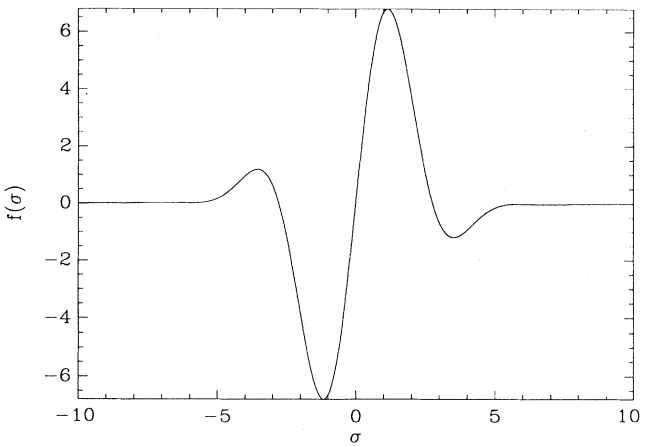

FIG. 1. Profile of $f(\sigma)=(v_{x10}v_{x10}^{*\prime\prime})'+\text{c.c.}$, where $v_{x10}(\sigma)$ is given by Eq. (15) and the prime denotes derivatives with respect to σ. This particular plot has been computed for $C=1$, $A_1=1$, and $\ln\epsilon^{1/3}=-5$.

The magnetic field components B_{x1} and B_{y1} are expanded in a manner similar to v_{x1} and v_{y1}, respectively. Inserting Eqs. (9)–(12) into Eq. (4) and combining the highest-order terms, we find that v_{x10} is governed by

$$\frac{d^4v_{x10}}{d\sigma^4} + iA_1\frac{d}{d\sigma}\left[\sigma\frac{dv_{x10}}{d\sigma}\right] = 0 . \quad (13)$$

The component v_{y10} can be computed in terms of v_{x10} using

$$v_{y10} = \frac{i}{k_y}\frac{dv_{x10}}{d\sigma} . \quad (14)$$

The solution of Eq. (13) that asymptotically matches the exterior region solution is [10]

$$v_{x10} = C\left[\int_0^\infty \frac{dp}{p}\exp\left[-\frac{p^3}{3|A_1|}\right](1-e^{i\,\text{sgn}(A_1)p\sigma}) + \ln\epsilon^{1/3}\right] . \quad (15)$$

Computing v_{y10} using Eq. (14) and B_{x10} and B_{y10} using Eq. (2) and inserting them in Eq. (6), we find that the highest-order contribution to $J_{z2}^{(0)}$ is given by

$$J_{z2}^{(0)} = -\frac{k_z}{\epsilon k_y}\frac{d}{d\sigma}\left[v_{x10}\frac{d^2v_{x10}^*}{d\sigma^2}\right] + \text{c.c.} \quad (16)$$

Using Eq. (15), it can be ascertained that the current density has odd symmetry about $\sigma=0$. We have plotted the profile of $J_{z2}^{(0)}$ in Fig. 1 after combining Eqs. (15) and (16) and numerically evaluating the definite integrals. From this figure it can be observed that the current is primarily localized within two closely spaced layers. The current density within these layers has equal magnitude but opposite polarity. Because of this odd symmetry, the total current in the resonance region is zero. We can use Eq. (5) to calculate the leading-order contribution to $B_{y2}^{(0)}$. It is given by

$$B_{y2}^{(0)}=-\frac{k_z C^2}{\epsilon^{2/3}k_y}\left[\int_0^\infty \frac{dp}{p}e^{-p^3/3|A_1|}(1-e^{i\,\mathrm{sgn}(A_1)p\sigma})+\ln\epsilon^{1/3}\right]\left[\int_0^\infty dp\,pe^{-p^3/3|A_1|}e^{-i\mathrm{sgn}(A_1)p\sigma}\right]+\text{c.c.} \tag{17}$$

The associated steady-state magnetic field is even about $\sigma=0$ and confined within a thin layer. We have plotted $B_{y2}^{(0)}$ in Fig. 3 after numerically solving Eqs. (1) and (2). From the expression for $B_{y2}^{(0)}$, we find that the amplitude and direction of the magnetic field are dependent on the primary wave amplitude and wave numbers. The amplitude and direction of the field within the layer can therefore be easily controlled externally. The position of the layer is also dependent, and hence controllable, by means of k_z. We make the additional observation that if the primary wave has several spectral components, each component will generate one such magnetized layer within the plasma and the total steady-state magnetic field will be a sum of the fields in the individual layers. The nonlinear interaction of the different spectral components can be neglected in this situation since the magnetic fields resulting from these interactions will vary harmonically in z or t and hence average to zero.

IV. NUMERICAL SOLUTION AND APPLICATIONS

The above three attributes of the magnetized layer make it a valuable tool that can be used for the synthesis or modification of transverse magnetic fields. In order to illustrate these applications, we numerically solve

$$AB_{x1}=i\rho_0\epsilon\mathcal{L}B_{x1}+ik_z\frac{dB_{z1}}{dx}\,, \tag{18}$$

$$AB_{y1}=i\rho_0\epsilon\mathcal{L}B_{y1}-k_yk_zB_{z1}\,, \tag{19}$$

$$\rho_0B_{z1}=ik_z\frac{dB_{x1}}{dx}-ik_zB_{x1}\frac{\rho_0'}{\rho_0}-\frac{d^2B_{z1}}{dx^2}+\frac{\rho_0'}{\rho_0}\frac{dB_{z1}}{dx}$$
$$-k_yk_zB_{y1}+k_y^2B_{z1}+i\epsilon\rho_0\mathcal{L}B_{z1}\,, \tag{20}$$

as a boundary value problem in a plasma slab extending from $x=-a$ to a. Equations (18)–(20) can be derived from Eqs. (1) and (2) and they have been found convenient for numerical solution. In the solution, it is assumed that

$$\rho_0(x)=\rho_{0(\max)}-[\rho_{0(\max)}-\rho_{0(\min)}]\left[\frac{x}{a}\right]^2,$$

where $\rho_{0(\min)}$ and $\rho_{0(\max)}$ are constants. Also, keeping in mind the symmetry of the equilibrium quantities, we assume that B_{x1} is odd about $x=0$ while B_{y1} and B_{z1} are even. It is found with the numerical solutions that fields in the interior are not sensitive to the values of B_{x1} and B_{y1} at the boundaries. Within a very thin boundary layer, the fields connect to relatively slowly varying values that are dependent only on $B_{z1}(x=\pm a)$. The boundary conditions that we use are therefore $B_{x1}(x=\pm a)=0$, $B_{y1}(x=\pm a)=0$, and $B_{z1}(x=\pm a)=$const. In the accompanying diagrams, Figs. 2–4, the fields within these boundary layers are not plotted since we are primarily interested in the behavior in the resonance region. Figure 2 shows the profile of steady-state current density in one-half of the plasma slab. It can be observed that the profile of the current density is similar to Fig. 1, which was computed using Eqs. (15) and (16). There is, however, a minor degree of asymmetry that gives rise to a small net integrated current [6,7]. Figure 3 shows the steady-state transverse magnetic field for the same situation. The slight asymmetry of the current density carries over to the magnetic field as well. As described earlier, the field is unidirectional and confined within a thin layer. Using the method of Kappraff and Tataronis [9], it can readily be shown that the width of the resonance layer is of the order of 1 cm for Pheadrus-T-like equilibrium parameters [11]. Let us now assume that in the plasma there is a series of magnetized layers that partially overlap. The field within these individual layers will add up and the result will be a transverse magnetic field with a profile that spans a wider region. Depending on the number of magnetized layers that are present, the magnetic field can span a portion of the complete plasma slab. To illustrate this, we have shown in Fig. 4 the total magnetic field that is created using an $O(\delta)$ wave with 27 spectral components, each having the same frequency but different wave numbers. Such a wave can be excited in the plasma using an appropriate external antenna with multiple components in the wave spectrum. Notice that the total magnetic field has a smooth profile and spans the whole plasma width. By changing the interspacing between the magnetized layers and their relative ampli-

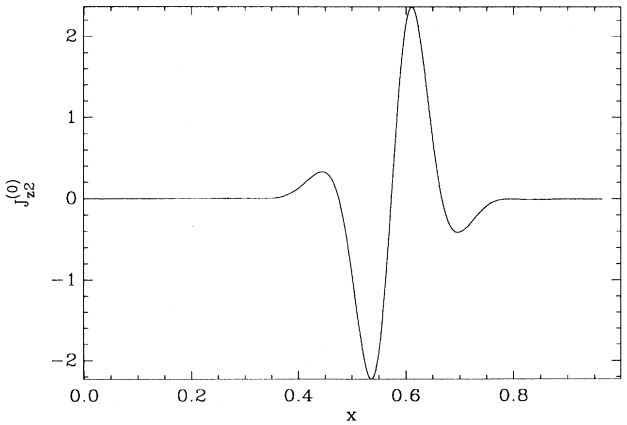

FIG. 2. Plot of $J_{z2}^{(0)}$ obtained from the numerical solution of Eqs. (18)–(20). The values of parameters that have been used in the computation are $a=1.05$, $\rho_{0(\min)}=0.8877$, $\rho_{0(\max)}=1.02$, $k_y=0.5$, $k_z=0.99$, $B_{z1}(x=a)=0.002$, $\epsilon=10^{-5}$, and $\Delta x=1.05/1000$.

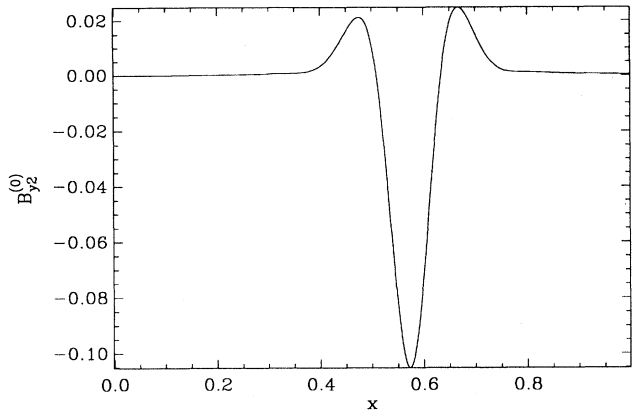

FIG. 3. Plot of $B_{y2}^{(0)}$ obtained from the numerical solution of Eqs. (18)–(20). The values of parameters that have been used in the computation are $a=1.05$, $\rho_{0(\min)}=0.8877$, $\rho_{0(\max)}=1.02$, $k_y=0.5$, $k_z=0.99$, $B_{z1}(x=a)=0.022$, $\epsilon=10^{-5}$, and $\Delta x=1.05/1000$.

tudes, the profile of this magnetic field can very easily be modified. The magnetic field generated in this manner can be used to modify already existing profiles as well as synthesize new ones.

V. EFFECT OF VISCOSITY

Until now, we have concentrated on a purely resistive plasma. We now analytically examine the effect of viscosity on the steady-state longitudinal current by assuming that γ and ϵ are of the same order. This situation requires the introduction of two additional boundary layers in the resonance region to take into account the highest derivative terms in Eq. (4). We also introduce a constant $\beta=\gamma/\epsilon$, which reduces the number of small parameters

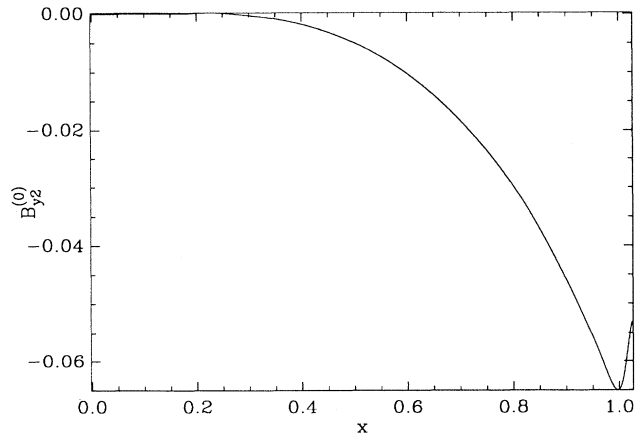

FIG. 4. Total steady-state magnetic field generated by exciting an $O(\delta)$ wave with 27 spectral components, each having the same frequency but different wave numbers. The parameters that are used in this computation are $a=1.05$, $\rho_{0(\min)}=0.8877$, $\rho_{0(\max)}=1.02$, $k_y=0.5$, $\epsilon=10^{-5}$, and $\Delta x=1.05/500$. The wave numbers k_z and amplitude $B_{z1}(x=a)$ for the spectral components are $k_{z(m)}=1.01-0.003m$ and $B_{z1(m)}(x=a)=0.0001m$, where $m=0,1,\ldots,26$.

to one. In the exterior regions, dissipative effects are negligible and v_{x1} is governed by Eq. (7). Its solution is given by Eq. (8). On the outer periphery of the resonance region where $x-x_0=O(\epsilon^{1/3})$, the leading-order terms in Eq. (4) balance with the terms multiplied with ϵ. Using the scaled variable σ and the asymptotic expansion described in Eqs. (9)–(12), we find that v_{x10} is governed by Eq. (13) with A_1 now replaced by $A_1/(1+\beta)$. The solution that asymptotically matches the exterior region solution is Eq. (15) with σ replaced by $\sigma/(1+\beta)^{1/3}$. This viscosity-induced rescaling signifies a broadening of the resonance region. When the plasma was purely resistive, the "intermediate" region solution was extended to $x=x_0$. the problem is, however, complicated in a viscoresistive plasma due to the fact that the highest derivative term in Eq. (4) is multiplied by ϵ^2. In the region near the resonance layer where $x-x_0=O(\epsilon^{1/2})$, the highest derivative terms in Eq. (4) balance with the terms multiplied by ϵ. To take this into account, we define an interior region with a width of order $\epsilon^{1/2}$ and introduce a scaled variable $\sigma'=\epsilon^{-1/2}(x-x_0)$ there. Expanding the equilibrium and wave components in a manner similar to Eqs. (9)–(12) (with σ replaced by σ' and $\epsilon^{1/3}$ replaced by $\epsilon^{-1/2}$) and inserting this expansion in Eq. (4), we find that v_{x10} is governed by

$$\frac{d^4}{d\sigma'^4}\left[\beta\frac{d^2}{d\sigma'^2}+i(1+\beta)\right]v_{x10}=0\ . \tag{21}$$

Retaining only the terms in the solution that do not exponentially increase as we leave the resonance surface and matching them asymptotically to the solution in the intermediate region, we obtain

$$v_{x10}=C[\ln\epsilon^{1/3}-iP_1\sigma'+P_2\sigma'^2+i\sigma'^3\epsilon^{1/2}A_1/6]\ , \tag{22}$$

where $P_1=\epsilon^{1/6}\Gamma(\frac{1}{3})\mathrm{sgn}(A_1)|A_1|^{1/3}/3^{2/3}$ and $P_2=\epsilon^{1/3}\Gamma(\frac{2}{3})(3|A_1|)^{2/3}/6$. The first-order fields can be used to compute $J_{z2}^{(0)}$ and $B_{y2}^{(0)}$. In the intermediate regions, $J_{z2}^{(0)}$ is given by Eq. (16) and $B_{y2}^{(0)}$ by Eq. (17). In the interior region, $J_{z2}^{(0)}$ is governed by an expression similar to Eq. (16) with ϵ replaced by $\epsilon^{3/2}$ and σ replaced by σ'. However, if we substitute Eq. (22) into this expression, we find that $J_{z2}^{(0)}$ is zero in the interior region. Consequently, using Eq. (5), $B_{y2}^{(0)}$ is constant there. The second effect of viscosity is therefore a flattening of the magnetic field within the resonance layer.

VI. CONCLUSIONS

In conclusion, we have examined the steady-state magnetic field that is generated by the nonlinear mixing of linear Alfvén waves in the vicinity of the Alfvén resonance surface. It was shown that this magnetic field is unidirectional and is confined within a thin layer. Furthermore, by using an antenna with multiple spectral components, a whole series of these magnetized layers can be created in the plasma. This feature can be utilized for the modification or synthesis of transverse magnetic fields. The present analysis has been carried out in a slab geometry. Similar results will also be obtained in a cylin-

drical plasma. Therefore, in principle, these techniques should be applicable to toroidal plasmas with a large aspect ratio. The problem, however, has to be reexamined for plasmas in which toroidal effects are strong.

ACKNOWLEDGMENT

This research was supported by the U.S. Department of Energy under Grant No. DE-FG02-88ER53264.

[1] T. Ohkawa, Comments Plasma Phys. Controlled Fusion **12**, 165 (1989).
[2] R. R. Mett and J. A. Tataronis, Phys. Rev. Lett. **63**, 1380 (1989).
[3] J. B. Taylor, Phys. Rev. Lett. **63**, 1385 (1989).
[4] V. S. Chan, R. L. Miller, and T. Ohkawa, Phys. Fluids B **2**, 944 (1990).
[5] S. Rauf and J. A. Tataronis, Bull. Am. Phys. Soc. **39**, 1624 (1994).
[6] R. R. Mett and J. B. Taylor, Phys. Fluids B **4**, 73 (1992).
[7] B. P. Pandey, K. Avinash, P. W. Kaw, and A. Sen, Phys. Plasmas **2**, 629 (1995).
[8] J. A. Tataronis and W. Grossmann, Z. Phys. **261**, 203 (1973).
[9] J. M. Kappraff and J. A. Tataronis, J. Plasma Phys. **18**, 209 (1977).
[10] J. M. Davila, Astrophys. J. **317**, 514 (1987).
[11] S. Wukitch, M. Vukovic, R. Breun, D. Brouchous, D. A. Diebold, M. Doczy, A. Elfimov, D. Edgell, N. Hershkowitz, T. Intrator, M. Kishinevsky, C. Litwin, P. Moroz, and P. Probert, Phys. Rev. Lett. **74**, 2240 (1995).